CMUG CCI+ Deliverable

Number: D2.0i
Interim report
Submission date: 27 April 2026
Version: 1.2

Climate Modelling User Group [CMUG]

Deliverable D2.0i

Interim Progress Report

Centres providing input: Met Office (R. King, D. Hemming)
CMCC (D. Peano, M. Mastropierro, B. Cardeli)

Version nr.	Date	Status
1.0	27 March 2026	Initial outline and first text.
1.2	27 April 2026	Version submitted to ESA

Deliverable D2.0i

Interim Progress Report

Contents

1. Introduction

Hydrometeorological processes regulate the exchange of water and energy between the land surface and the atmosphere. Vegetation plays an important active role in these exchanges through its phenology, structure, and functional traits. These properties influence surface albedo, rooting depth, evapotranspiration, and hence the land surface temperature and soil moisture. The vegetation dynamics respond to the variability in hydrometeorological conditions such as precipitation, surface runoff, and atmospheric water vapour, which control the water availability, meaning understanding these relationships is an important step in vegetation modelling within climate models.

This work explores the relationship between vegetation phenology and hydrometeorological quantities, focusing on how their interactions evolve across space and time. These interactions can exert a strong control on the surface conditions, and can amplify or dampen climate extremes through land-atmosphere feedbacks. Examples of this include the intensification of heat and drought conditions during the 2003 European heatwave (Ciais et al., 2005), and the role of changing vegetation in the resilience of the Amazon basin (Zemp et al., 2017).

Spatio-temporal variations in vegetation cover and traits influence water, heat and carbon exchanges, with some locations and phenology event timings showing stronger sensitivities to changes in the vegetation properties than others. It is important to understand and model these relationships and sensitivities, and how they vary across spatio-temporal scales, to enable continued advances in the modelling of hydrometeorological processes within Earth system models (ESMs) and inform sustainable land use management into the future.

This report begins with detailing the European Space Agency (ESA) Climate Change Initiative (CCI) Essential Climate Variables (ECVs) data that are used in this analysis, along with the other sources of observation data and Coupled Model Intercomparison Project phase 6 (CMIP6) (Eyring et al., 2016) model data evaluated. A review of the phenology metrics being used is given in section 3 along with the plans and progress towards an ESMValTool diagnostic. Section 4 introduces the hydrometeorological relationship between water vapour and soil moisture. The final section outlines the plans for this work package to combine the phenology and hydrometeorology methods and results into a combined set of relationships.

2. Essential Climate Variables

This study focuses on vegetation phenology and its relationship with hydrometeorological processes. The primary source of observation data is from ESA CCI ECVs. The ECVs used in results presented here, and those planned to be used, are listed in Table 1. Feedback for the CCI providers was previously given in Deliverable 5.2.5 (available from ESA), and this will be updated throughout this work package.

Table 1: Essential Climate Variables (ECVs) from Climate Change Initiative (CCI) teams, and the release version used in this OWP5.9 CMUG study. Those highlighted in grey have been in results presented in this report, with the remaining planned to be used.

CCI Team	Version	Variable
Vegetation	1.0	Leaf Area Index (LAI)
Soil Moisture	9.1	Gap-filled version
Water Vapour	3.2	Total Column Water Vapour (TCWV)
Land Cover	2.0.8	Plant Functional Types distribution
Snow	3.1	Snow water equivalent
Land surface temperature	4.0, 5.11	Land surface temperature
Biomass	5.0.1	Above ground biomass

Phenology Observation Sources

Other sources of observation data are used to complement the CCI data. Green Chromatic Coordinate (GCC) data are taken from PhenoCam[1]. GCC is the ratio of green digital counts to the sum of the individual red, green and blue digital counts in a digital photograph, or region of such an image,

$$GCC = \frac{G}{R + G + B}$$

where R, G, and B are the digital count values of the red, green and blue pixels respectively. GCC is used as a measure of greenness, as a proxy for how much of the image consists of green leaves. Equivalently, Red Chromatic Coordinate (RCC) looks at the redness of the image. RCC has potential to be used to evaluate offset (end of the growing season) dates, marking the end of the growing season, by peaking at that time due to the leaf colour changes in autumn.

An example of the annual cycle of GCC and RCC is shown in Figure 1 for the PhenoCam site at Monte Bondone, Italy. The GCC follows a similar curve to that expected of LAI. The RCC shows, amongst other features, a peak at the end of the growing season associated with the breakdown of the green chlorophyll, allowing the colour of xanthophylls and carotenoids to be seen, in addition to the release of anthocyanins in the leaves.

[1] https://phenocam.nau.edu/webcam/

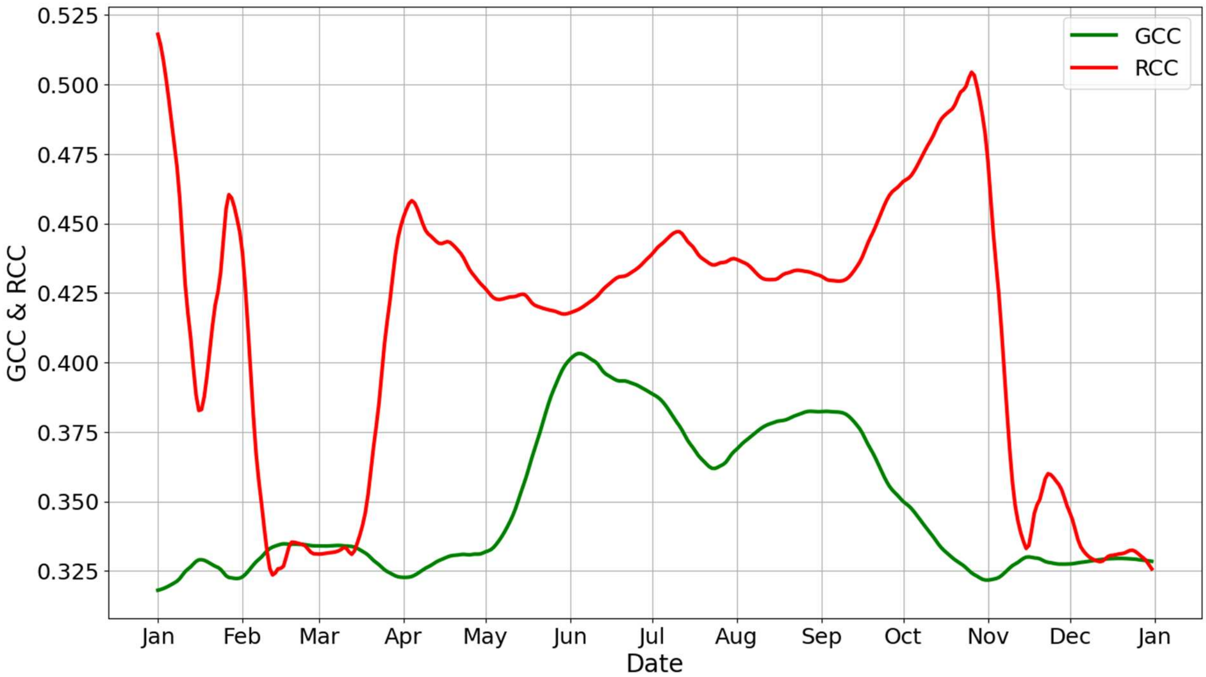

Figure 1: The green chromatic coordinate (GCC) and red chromatic coordinate (RCC) at the Monte Bondone grass PhenoCam site for 2017. The GCC (green curve) shows onset during May and offset in October. The RCC (red curve) shows a marked increase during September into October, indicative of offset occurring during this period.

Other Observation Sources

Observations of precipitation are being considered from the Global Precipitation Climatology Project (GPCP) (Schneider et al., 2014), a rain gauge and satellite combined product, and the Tropical Rainfall Measuring Mission (TRMM) (Barnes et al., 1998), a satellite-based product. For surface runoff and evapotranspiration, the Global Runoff Data Centre (GRDC) (GRDC web site), and the Moderate Resolution Imaging Spectroradiometer (MODIS) evapotranspiration MOD16[2] product are being explored. Data and advice will be sought from the new CCI Land Evaporation group.

Model and Reanalysis Data

Results in this study are used to evaluate models from CMIP6 (Eyring et al., 2016). Data are taken from the following models:

- UKESM (Sellar et al., 2019)
- CMCC-ESM2 (Lovato et al., 2022)
- MPI-ESM1-2-HR (Gutjahr et al., 2019)
- IPSL-CM6A-LA-INCA (Boucher et al., 2020)
- NorESM2-LM (Seland et al., 2020).

[2] https://modis.gsfc.nasa.gov/data/dataprod/mod16.php

Further climate model data are planned to be used from the Land Use Model Intercomparison Project (LUMIP) (Lawrence et al., 2016), and the Land Surface, Snow and Soil Moisture Intercomparison Project (LS3MIP) (Van Den Hurk et al., 2016).

ERA5 (Hersbach et al., 2020) and ERA5-Land (Muñoz-Sabater et al., 2021) reanalysis data are planned to provide global coverage of hydrometeorological quantities such as runoff, precipitation and atmospheric moisture.

3. Phenology Metrics and Methods

Leaf Area Index Data Cleaning

The CCI LAI data (Version 1) require a pre-processing phase to remove LAI values attached to a high uncertainty, remove outliers, and to gap fill and smooth the timeseries. The full method is detailed in Deliverable D3.1b (available from ESA), and the outline is given here:

1. **Filter high uncertainty:** Remove LAI values that have Standard Error > 1.
2. **Noise reduction:** Use the z-score to filter LAI values with z-score > 95th percentile of the entire timeseries' z-score.
3. **Gap fill:** Use linear regression to fill gaps in the original data and those created in steps 1 and 2.
4. **Smoothing:** A Savitzky-Golay filter is applied to the gap filled timeseries, 3rd order polynomial and window width of 19 timesteps, to create the final filled and smoothed timeseries.

Vegetation Onset

Vegetation phenology metrics describe the timing and magnitude of phenophases, events in the vegetation's life cycle. It is important that climate models accurately capture these events to correctly model the carbon and water cycles. Recent studies, e.g. (Peano et al., 2019), (Peano et al., 2021) and (Li et al., 2022), show that state-of-the-art land surface models (LSMs) simulate a delay in several phenophases, such as start, peak, and end of the vegetation's active season. These results highlight a generalised delay of the plant growing season in LSMs.

The start of the growing season (in deciduous regions) is marked by the appearance of leaves, and the associated greening of the wider area. This has several terms with similar meaning such as start-of-season, vegetation onset, and leaf up. Here, vegetation onset, or just *onset*, is used to mean this event.

Leaf area index is used to derive the day of the year onset occurs. A threshold value of LAI, representing a defined area of leaves on the vegetation, gives the point onset is considered to occur. Similarly, GCC as proxy for leaf cover and hence LAI, can also be used to derive a date onset occurred. The two variables LAI and GCC represent different observation length scales and hence may give different dates for onset or require different threshold values to accurately capture the onset date.

The method of (Peano et al., 2019) is used to determine the onset from LAI and GCC data. LAI is available as a prognostic variable in Land Surface Models (LSMs), for example (Peano et al., 2019). GCC is observed in-situ and gives a measure of the leaf cover across the region of interest in the underlying images. The dates of onset can be compared between the two variables to understand how well both satellite observations (LAI) and CMIP6 models capture events as measured at site level.

Onset is defined as the date the LAI (or GCC) first exceeds a critical threshold, CT,

$$CT = LAI_{min} + \alpha(LAI_{max} - LAI_{min})$$

where LAI_{min} and LAI_{max} are the minimum and maximum value of LAI (GCC) in the year, and α is a parameter to determine. The value $\alpha = 0.20$ is used in (Peano et al., 2019) for LAI, and a range of values for α are discussed in Deliverable D3.1b (available from ESA) for LAI and GCC, and also in (Kang et al., 2003). Figure 2 shows this process for calculating the onset date from GCC at the Arbutus Lake PhenoCam site.

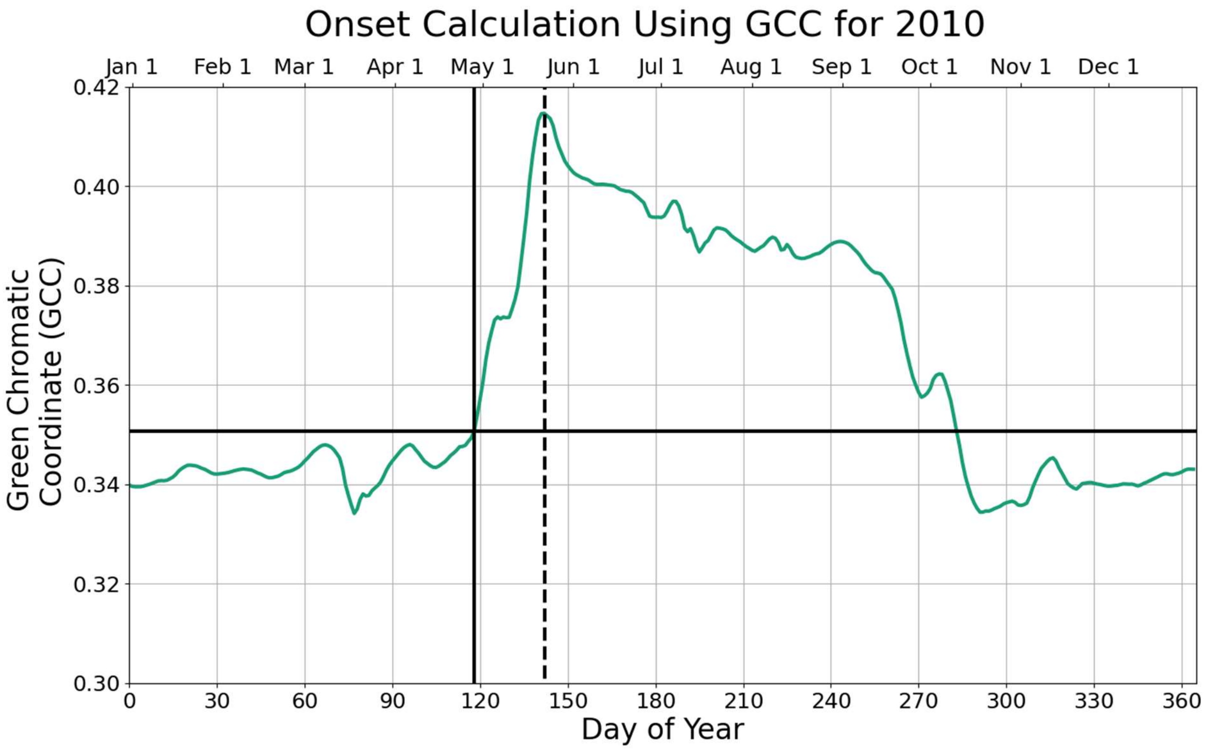

Figure 2: The Green Chromatic Coordinate (GCC) for 2010 at the Arbutus Lake PhenoCam site. The process for calculating the onset date is illustrated: The dashed line shows the peak GCC value, meaning onset will be earlier than this date. The black crosshair shows the critical threshold (CT) of GCC using $\alpha = 0.20$ *and the date the timeseries first exceeds this. This gives an onset date as 29th April (day 119 of the year). The local minima at day 77 is an example of values affecting the* LAI_{min} *value potentially giving an earlier onset date, discussed in Section 5.*

Identifying Growing Season Types

The seasonal cycle of LAI can be used to classify how the vegetation grows throughout the year. The number of growing seasons in a year, and the timing of these growing seasons, can be used to classify regions, and the spatial distribution of these regions can be compared from those derived from satellite data to those derived from model data. One such classification method is the four growing season type (4GST) (Peano et al., 2019).

The 4GST method classifies regions based on whether there are zero, one, or two distinct growing seasons and further sub-classifies the one growing season type based on the time of the year it occurs:

1. Evergreen (EVG),
2. Single Growing Season with Summer Peak (SGS-S),
3. Single Growing Season with Summer Dormancy (SGS-D),
4. Two Growing Seasons (TGS).

Evergreen

Regions with the EVG type are characterised by a limited variation in canopy density, for example (Wu et al., 2014), manifesting as a low variability in the LAI. This variability in one year can be calculated using the minimum, maximum and mean LAI values, LAI_{min}, LAI_{max}, and LAI_{mean} respectively. The variability is calculated as below and a value ε is chosen as a threshold.

$$\frac{LAI_{max} - LAI_{min}}{LAI_{mean}} < \varepsilon \Rightarrow EVG$$

When the left-hand side is less than ε, the region is classified as evergreen, EVG. A value of $\varepsilon = 0.25$ is used in (Peano et al., 2019).

Single Growing Season

Once it has been established that a region is not EVG, then it is tested to determine which of the two single growing season types, or two growing season type applies. The first step in the method is to recentre the year's LAI timeseries on the maximum value, wrapping values as necessary. The timeseries is next divided into four periods of three months plus the 15 days either side. Finally, for each of these four periods, the sign of the slope of the linear regression of the LAI values is calculated.

This gives a sequence of four signs, + or -. The sequence can take two forms for the region to be a single growing season, [++--] and [--++]. The former is a summer growing type, SGS-S, the later SGS-D a summer dormancy type in the Northern hemisphere and reversed for the Southern hemisphere.

Two Growing Seasons

Following the procedure for single growing seasons, a sequence of + and – that does not correspond to either of the SGS types. These sequences are [+-+-] and [-+-+] and correspond to two growing seasons for the region, TGS.

ESMValTool

ESMValTool is a community diagnostic tool for evaluating Earth system models (ESMs) (Eyring et al., 2020). It allows observation data and ESM output to be compared, and metrics and other evaluation types to be performed. The data preparation and collection are controlled by recipes, and metrics and scientific output are written in diagnostics.

A recipe and diagnostic are being written to implement the 4GST method into ESMValTool[3]. These will read the Copernicus LAI data (Blessing & Giering, 2010) initially and is planned to implement CCI LAI data into ESMValTool once version 2 of this dataset is available.

The procedure and calculations of the 4GST classifications are agnostic to the source of the LAI data. This means that the final diagnostic will be able to make comparisons of observation data to historic simulations from CMIP6, comparisons of multiple CMIP6 models and experiments to each other, and perform investigations into changes of a region's classification under different future scenarios.

4. Relationship between Water Vapour and Soil Moisture

The relationship between atmospheric water vapour and soil moisture is assessed by investigating the correlation between the two variables along the transect of the available CCI LAI (version 1) data. Atmospheric water vapour is taken from the CCI total column water vapour (TCWV) product, and soil moisture from the gap-filled version of the CCI soil moisture (SM) product.

The daily TCWV was resampled to monthly values, and anomalies considered for both TCWV and SM to exclude seasonal trends. The monthly mean aggregation of TCWV is necessary to have at least one data point per gridbox in the studied region. This avoids data gaps in regions where daily satellite overpasses are rarer, such as the tropics.

Pearson R coefficient values are shown in Figure 3 for the four seasons. Most of the regions do not show any trend or pattern, demonstrating the weak hydrological coupling between land (soil moisture) and atmosphere (water vapour) at the monthly and seasonal timescales. This is mostly expected because the land-atmosphere hydrological coupling is evident and relevant on a daily/weekly basis, which corresponds to the timescales of soil moisture response to rainfall events, and to the evapotranspiration influence on atmospheric water vapour.

[3] Github issue: https://github.com/ESMValGroup/ESMValTool/issues/4405

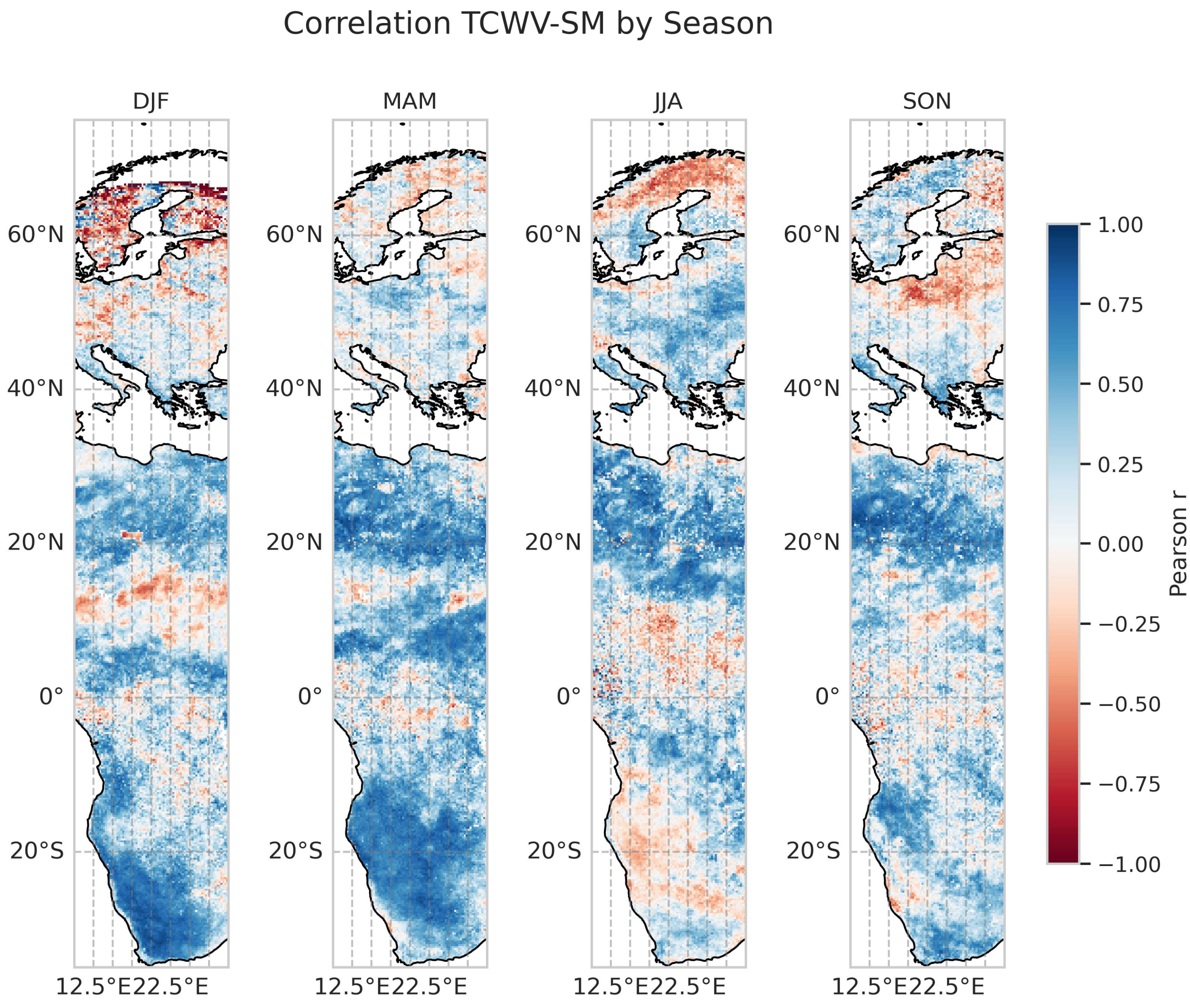

Figure 3: Seasonal correlation plots of total column water vapour (TCWV) and soil moisture anomalies shown for the area covered by the transect of CCI LAI data. Left to right are winter (December, January, February), spring (March, April, May), summer (June, July, August) and autumn (September, October, November), using the Northern hemisphere timings. The colour represents the Pearson R coefficient, ranging from red at R=-1 through to blue at R=1.

Despite this apparent global limitation, certain regions do exhibit a stronger land-atmosphere coupling using this metric. Notably a region in south-western Africa bounded by latitude 10° South to 25° South, and longitude 12.5° East to 20° East, consisting of a dryland grass ecosystem, displays a stronger response of SM to TCWV. Using the CCI Land Cover product, only those grid boxes where the grass coverage is greater than 90% are considered. This isolates the signal originating from the grassland modulation of SM-TCWV interaction. Figure 4 shows a marked seasonality in this region, with positive correlation coefficient values especially for summer (December, January, February) and autumn (March, April, May), and negative correlation values for winter (June, July, August). This pattern could be linked to the climatological seasonal cycle in precipitation over the investigated region, which is characterised by low to no precipitation during winter and higher precipitation in summer, e.g. (Pereira et al., 2024)

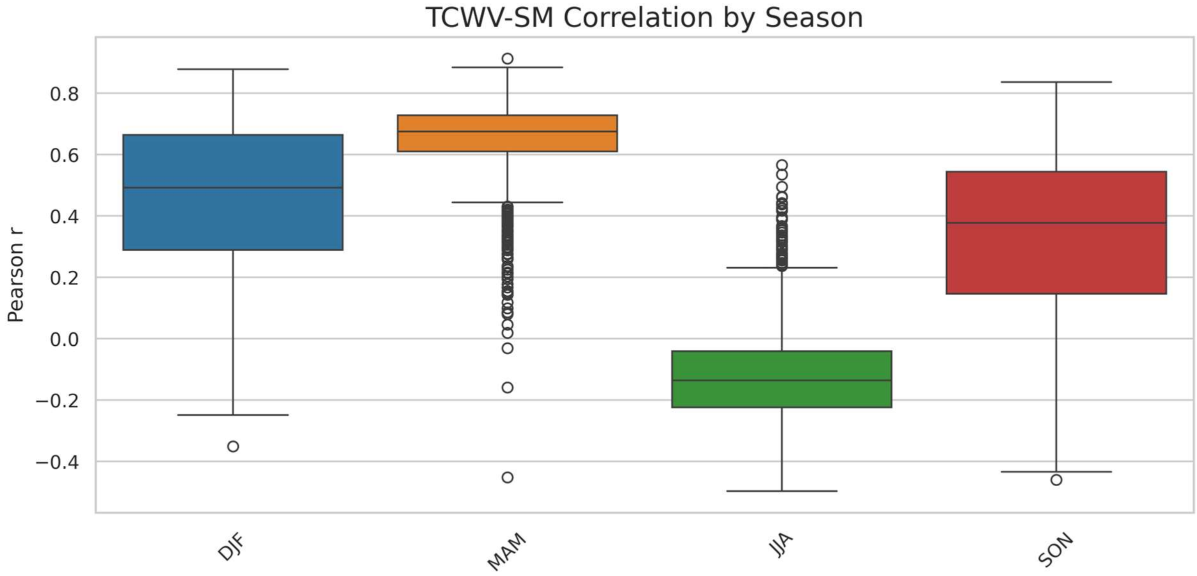

Figure 4: Seasonal correlation plots of total column water vapour (TCWV) and soil moisture anomalies in the southern African region bounded by 10° South to 25° South, and longitude 12.5° East to 20° East. The box represents the inter-quartile range (25^{th}-75^{th} percentile), central line the median value, the whiskers the 5^{th} and 95^{th} percentiles, and circles are all data points outside of the 5^{th}-95^{th} percentile range.

5. Future Plans

This work is planned to proceed along two lines which will be combined to give the final results. First, to write a diagnostic for ESMValTool to compute phenology metrics, namely the 4GST and onset dates. This work complements the ESMValTool CMORiser for Copernicus LAI data from CMUG work package 4.3. Alongside this, techniques to make best use of the high frequency LAI data for metrics such as onset will be applied. This is to reduce the impact of noise creating anomalous values, for example in the case of a local minimum value incorrectly being used as the global minimum value when calculating the critical threshold in the onset calculation as shown in Figure 2. This will improve the 4GST method for calculating phenology metrics because the original use utilised data at lower time frequencies where such events and noise in the timeseries are naturally smoothed and not exposed to the user.

Secondly, the relationships between water vapour and other hydrometeorology quantities will continue to be developed. This will be for both observations and in CMIP6 models. Additional parameters are planned to be introduced into the analysis such as total precipitation, runoff, and evapotranspiration. The use of Global Land Evaporation Amsterdam Model (GLEAM) (Miralles et al., 2025) and the new ESA CCI Land Evaporation project[4] are planned to be explored to provide data and analysis on latent and sensible heat fluxes.

[4] https://climate.esa.int/en/projects/Land-Evaporation/

Finally, the phenology and hydrometeorology results will be combined. This is to assess the relationship between the timing of phenology events and the nature of the relationship between the hydrometeorology quantities.

6. References

Barnes, W., Shiue, J., & Simpson, J. (1998). *The Tropical Rainfall Measuring Mission (TRMM) Sensor Package*.

Blessing, S., & Giering, R. (2010). *Algorithm Theoretical Basis Document Multi-sensor CDR LAI and fAPAR v3.0*.

Boucher, O., Servonnat, J., Albright, A. L., Aumont, O., Balkanski, Y., Bastrikov, V., Bekki, S., Bonnet, R., Bony, S., Bopp, L., Braconnot, P., Brockmann, P., Cadule, P., Caubel, A., Cheruy, F., Codron, F., Cozic, A., Cugnet, D., D'Andrea, F., … Vuichard, N. (2020). Presentation and Evaluation of the IPSL-CM6A-LR Climate Model. *Journal of Advances in Modeling Earth Systems*, *12*(7). https://doi.org/10.1029/2019MS002010

Ciais, P., Reichstein, M., Viovy, N., Granier, A., Ogée, J., Allard, V., Aubinet, M., Buchmann, N., Bernhofer, C., Carrara, A., Chevallier, F., De Noblet, N., Friend, A. D., Friedlingstein, P., Grünwald, T., Heinesch, B., Keronen, P., Knohl, A., Krinner, G., … Valentini, R. (2005). Europe-wide reduction in primary productivity caused by the heat and drought in 2003. *Nature*, *437*(7058), 529–533. https://doi.org/10.1038/nature03972

Eyring, V., Bock, L., Lauer, A., Righi, M., Schlund, M., Andela, B., Arnone, E., Bellprat, O., Brötz, B., Caron, L. P., Carvalhais, N., Cionni, I., Cortesi, N., Crezee, B., Davin, E. L., Davini, P., Debeire, K., De Mora, L., Deser, C., … Zimmermann, K. (2020). Earth System Model Evaluation Tool (ESMValTool) v2.0 - An extended set of large-scale diagnostics for quasi-operational and comprehensive evaluation of Earth system models in CMIP. *Geoscientific Model Development*, *13*(7), 3383–3438. https://doi.org/10.5194/gmd-13-3383-2020

Eyring, V., Bony, S., Meehl, G. A., Senior, C. A., Stevens, B., Stouffer, R. J., & Taylor, K. E. (2016). Overview of the Coupled Model Intercomparison Project Phase 6 (CMIP6) experimental design and organization. *Geoscientific Model Development*, *9*(5), 1937–1958. https://doi.org/10.5194/gmd-9-1937-2016

GRDC. (GRDC web site). *Global Runoff Data Centre*. Https://Grdc.Bafg.De/.

Gutjahr, O., Putrasahan, D., Lohmann, K., Jungclaus, J. H., Von Storch, J. S., Brüggemann, N., Haak, H., & Stössel, A. (2019). Max Planck Institute Earth System Model (MPI-ESM1.2) for the High-Resolution Model Intercomparison Project (HighResMIP). *Geoscientific Model Development*, *12*(7), 3241–3281. https://doi.org/10.5194/gmd-12-3241-2019

Hersbach, H., Bell, B., Berrisford, P., Hirahara, S., Horányi, A., Muñoz-Sabater, J., Nicolas, J., Peubey, C., Radu, R., Schepers, D., Simmons, A., Soci, C., Abdalla, S., Abellan, X., Balsamo, G., Bechtold, P., Biavati, G., Bidlot, J., Bonavita, M., … Thépaut, J. N. (2020). The ERA5 global reanalysis. *Quarterly Journal of the Royal Meteorological Society*, *146*(730), 1999–2049. https://doi.org/10.1002/qj.3803

Kang, S., Running, S. W., Lim, J. H., Zhao, M., Park, C. R., & Loehman, R. (2003). A regional phenology model for detecting onset of greenness in temperate mixed forests, Korea: An application of MODIS leaf area index. *Remote Sensing of Environment*, *86*(2), 232–242. https://doi.org/10.1016/S0034-4257(03)00103-2

Lawrence, D. M., Hurtt, G. C., Arneth, A., Brovkin, V., Calvin, K. V., Jones, A. D., Jones, C. D., Lawrence, P. J., Noblet-Ducoudré, N. De, Pongratz, J., Seneviratne, S. I., & Shevliakova, E. (2016). The Land Use Model Intercomparison Project (LUMIP) contribution to CMIP6: Rationale and experimental design. *Geoscientific Model Development*, *9*(9), 2973–2998. https://doi.org/10.5194/gmd-9-2973-2016

Li, X., Melaas, E., Carrillo, C. M., Ault, T., Richardson, A. D., Lawrence, P., Friedl, M. A., Seyednasrollah, B., Lawrence, D. M., & Young, A. M. (2022). A Comparison of Land Surface Phenology in the Northern Hemisphere Derived from Satellite Remote Sensing and the Community Land Model. *Journal of Hydrometeorology*. https://doi.org/10.1175/JHM-D-21

Lovato, T., Peano, D., Butenschön, M., Materia, S., Iovino, D., Scoccimarro, E., Fogli, P. G., Cherchi, A., Bellucci, A., Gualdi, S., Masina, S., & Navarra, A. (2022). CMIP6 Simulations With the CMCC Earth System Model (CMCC-ESM2). *Journal of Advances in Modeling Earth Systems*, *14*(3). https://doi.org/10.1029/2021MS002814

Miralles, D. G., Bonte, O., Koppa, A., Baez-Villanueva, O. M., Tronquo, E., Zhong, F., Beck, H. E., Hulsman, P., Dorigo, W., Verhoest, N. E. C., & Haghdoost, S. (2025). GLEAM4: global land evaporation and soil moisture dataset at 0.1 resolution from 1980 to near present. *Scientific Data* , *12*(1). https://doi.org/10.1038/s41597-025-04610-y

Muñoz-Sabater, J., Dutra, E., Agustí-Panareda, A., Albergel, C., Arduini, G., Balsamo, G., Boussetta, S., Choulga, M., Harrigan, S., Hersbach, H., Martens, B., Miralles, D. G., Piles, M., Rodríguez-Fernández, N. J., Zsoter, E., Buontempo, C., & Thépaut, J. N. (2021). ERA5-Land: A state-of-the-art global reanalysis dataset for land applications. *Earth System Science Data*, *13*(9), 4349–4383. https://doi.org/10.5194/essd-13-4349-2021

Peano, D., Hemming, D., Materia, S., Delire, C., Fan, Y., Joetzjer, E., Lee, H., Nabel, J. E. M. S., Park, T., Peylin, P., Wärlind, D., Wiltshire, A., & Zaehle, S. (2021). Plant phenology evaluation of CRESCENDO land surface models-Part 1: Start and end of the growing season. *Biogeosciences*, *18*(7), 2405–2428. https://doi.org/10.5194/bg-18-2405-2021

Peano, D., Materia, S., Collalti, A., Alessandri, A., Anav, A., Bombelli, A., & Gualdi, S. (2019). Global Variability of Simulated and Observed Vegetation Growing Season. *Journal of Geophysical Research: Biogeosciences*, *124*(11), 3569–3587. https://doi.org/10.1029/2018JG004881

Pereira, C. A., Martins, J. P., Fink, A. H., Pinto, J. G., & Ramos, A. M. (2024). Drivers of seasonal rainfall variability over the Angolan and Namibian plateaus. *International Journal of Climatology*, *44*(11), 3706–3725. https://doi.org/10.1002/joc.8545

Schneider, U., Becker, A., Finger, P., Meyer-Christoffer, A., Ziese, M., & Rudolf, B. (2014). GPCC's new land surface precipitation climatology based on quality-controlled in situ data and its role in quantifying the global water cycle. *Theoretical and Applied Climatology*, *115*(1–2), 15–40. https://doi.org/10.1007/s00704-013-0860-x

Seland, Ø., Bentsen, M., Olivié, D., Toniazzo, T., Gjermundsen, A., Graff, L. S., Debernard, J. B., Gupta, A. K., He, Y. C., Kirkevåg, A., Schwinger, J., Tjiputra, J., Schanke Aas, K., Bethke, I., Fan, Y., Griesfeller, J., Grini, A., Guo, C., Ilicak, M., … Schulz, M. (2020). Overview of the Norwegian Earth System Model (NorESM2) and key climate response of CMIP6 DECK, historical, and scenario simulations. *Geoscientific Model Development*, *13*(12), 6165–6200. https://doi.org/10.5194/gmd-13-6165-2020

Sellar, A. A., Jones, C. G., Mulcahy, J. P., Tang, Y., Yool, A., Wiltshire, A., O'Connor, F. M., Stringer, M., Hill, R., Palmieri, J., Woodward, S., de Mora, L., Kuhlbrodt, T., Rumbold, S. T., Kelley, D. I., Ellis, R., Johnson, C. E., Walton, J., Abraham, N. L., … Zerroukat, M. (2019). UKESM1: Description and Evaluation of the U.K. Earth System Model. *Journal of Advances in Modeling Earth Systems*, *11*(12), 4513–4558. https://doi.org/10.1029/2019MS001739

Van Den Hurk, B., Kim, H., Krinner, G., Seneviratne, S. I., Derksen, C., Oki, T., Douville, H., Colin, J., Ducharne, A., Cheruy, F., Viovy, N., Puma, M. J., Wada, Y., Li, W., Jia, B., Alessandri, A., Lawrence, D. M., Weedon, G. P., Ellis, R., … Sheffield, J. (2016). LS3MIP (v1.0) contribution to CMIP6: The Land Surface, Snow and Soil moisture Model Intercomparison Project - Aims, setup and expected outcome. *Geoscientific Model Development*, *9*(8), 2809–2832. https://doi.org/10.5194/gmd-9-2809-2016

Wu, C., Gonsamo, A., Gough, C. M., Chen, J. M., & Xu, S. (2014). Modeling growing season phenology in North American forests using seasonal mean vegetation indices from MODIS. *Remote Sensing of Environment*, *147*, 79–88. https://doi.org/10.1016/j.rse.2014.03.001

Zemp, D. C., Schleussner, C. F., Barbosa, H. M. J., Hirota, M., Montade, V., Sampaio, G., Staal, A., Wang-Erlandsson, L., & Rammig, A. (2017). Self-amplified Amazon forest loss due to vegetation-atmosphere feedbacks. *Nature Communications*, *8*. https://doi.org/10.1038/ncomms14681

7. Glossary

Acronyms	
4GST	Four Growing Season Types
CCI	Climate Change Initiative
CMIP6	Climate Model Intercomparison Project- phase 6
CMOR	Climate Model Output Rewriter
CMUG	Climate Modelling Users Group
ECV	Essential Climate Variable
ERA	ECMWF Reanalysis
ESA	European Space Agency
EVG	Evergreen growing type
GCC	Green Chromatic Coordinate
GLEAM	Global Land Evaporation Amsterdam Model
GPCP	Global Precipitation Climatology Project
GRDC	Global Runoff Data Centre
LAI	Leaf Area Index
LS3MIP	Land surface, Snow and Soil moisture Model Intercomparison Project
LUMIP	Land Use Model Intercomparison Project
MODIS	Moderate Resolution Imaging Spectroradiometer

RCC	Red Chromatic Coordinate
SGS-D	Single Growing Season – summer Dormancy
SGS-S	Single Growing Season – Summer peak
SM	Soil Moisture
TCWV	Total Column Water Vapour
TGS	Two Growing Seasons
TRMM	Tropical Rainfall Measuring Mission